Rock Mech Rock Eng (2017) 50:1661–1666
DOI 10.1007/s00603-017-1185-3

TECHNICAL NOTE

High-Temperature Influence on Mechanical Properties of Diorite

Hong Tian[1] · Gang Mei[2] · Guo-Sheng Jiang[1] · Yan Qin[2]

Received: 26 June 2016 / Accepted: 6 February 2017 / Published online: 14 February 2017

Keywords Diorite · High temperature effects · Uniaxial compressive strength · Elastic modulus · Failure pattern

1 Introduction

Knowledge on rock mechanical behaviors under/after high-temperature conditions is extremely important for projects such as deep geological disposal of nuclear waste (Sellin and Leupin 2013; Verma et al. 2015), hot dry rock (HDR) geothermal energy extraction (Brown et al. 2012; Gelet et al. 2012), and underground coal gasification (Burton et al. 2006; Otto and Kempka 2015), for it can provide a basis for deformation, stability, and safety analyses of the projects. High temperatures can cause thermal expansion of rock-forming minerals, thermal stresses, and chemical reactions in a rock body and thus produces micro-cracks and damages rock microstructures. As a result, rock behaviors exposed to high temperatures may be quite different from those under normal temperature conditions. It has been known that rock strength and deformation modulus generally decrease with increasing temperature, especially beyond a certain temperature (e.g., Dwivedi et al. 2008; Chen et al. 2012; Singh et al. 2015; Tian et al. 2016; Peng et al. 2016; Ding et al. 2016). Therefore, research on high-temperature rock mechanics is important and essential in both theory and practice.

Granitic rocks such as granite and diorite are a widely acceptable site for nuclear waste disposal and are also main rock types of HDR reservoir. Up to now, a large amount of experimental research has been performed to investigate the mechanical properties of granite exposed to high temperatures up to 1000 °C. Dwivedi et al. (2008) presented deformation modulus, tensile, and compressive strength of granites basically decrease with temperature according to their experiments and literature review. Based on a real-time high-temperature uniaxial compression testing system with strain rates of 0.05 and 0.5 mm/min, Singh et al. (2015) found uniaxial compression strength (UCS) and elastic modulus (E) of granite decrease with temperature from 200 °C onward, while Homand-etienne and Houpert (1989), Chen et al. (2012) and Liu and Xu (2014) discovered the threshold temperature is 400 °C. They found granite UCS changes slightly from room temperature to 400 °C, but dramatically decreases with temperature from 400 °C onward, by means of testing on granite sample after high-temperature treatment. Shao et al. (2015) and Yin et al. (2016) observed UCS and E of granites decrease with temperature up to 1000 °C.

Diorite reserves may be much larger than that of granite in some areas and can be a substitute for granite as the host rock of nuclear waste geological disposal. It is also one type of hot dry rocks. However, limited reference related to the mechanical behavior of diorite exposed to high temperatures is available now. To extend our knowledge on high-temperature influences on mechanical properties of diorite, a series of uniaxial compression tests were performed on diorite samples after thermal treatment up to 1000 °C.

✉ Gang Mei
gang.mei@cugb.edu.cn

[1] Faculty of Engineering, China University of Geosciences, Lumo Road 388, Wuhan, China

[2] School of Engineering and Technology, China University of Geosciences, Xueyuan Road 29, Beijing 100083, China

2 Materials and Methods

2.1 Sample Characterization

Block samples in this study are gray compact diorite retrieved from the Fangshan District, Beijing, China. According to the Standard for Tests Method of Engineering Rock Messes (GB/T 50266-99) of the Peoples Republic of China, cylindrical specimens with a nominal diameter of 50 mm and length to diameter ratio of two were prepared for uniaxial compression testing. The average bulk density, open porosity, and compressive wave velocity of the original samples are 2.70 g/cm^3, 1.02%, and 3491 m/s, respectively. The average values of UCS, E and Poisson's ratio of the samples without thermal treatment are 46.7 MPa, 12.6 GPa, and 0.1, respectively. The mineral composition is about 45% plagioclase, 25% K-feldspar, 10% quartz, 10% amphibole, and 10% biotite by weight percent.

2.2 Testing Procedure

To eliminate the influences of natural water content on the experimental results, all the samples were first numbered and subjected to dry processing which is performed by putting the samples into a drying oven and baking them at 105 °C for 48 h to remove all moisture content. And then, thermal treatment was performed on the dried samples in an electrical furnace (SG-XL1200) with the following procedure:

- heat the dried samples at a rate of 2 °C/min at atmospheric pressure to a predetermined temperature in the furnace chamber;
- maintain the samples at the predetermined temperature for 2 h;
- cool them down in the chamber at a rate of 2 °C/min to room temperature.

After that, the treated samples were conserved in a desiccator until uniaxial compression testing. The predetermined temperatures were 200, 400, 600, 800, and 1000 °C, respectively.

Following the standard of GB/T 50266-99, the uniaxial compression experiments were carried out at a loading speed of 0.3 mm/min in a TAW-2000 electric-fluid servo-controlled testing system as shown in Fig. 1. Three samples were used for the testing at each temperature level.

Fig. 1 Photograph showing the TAW-2000 servo-controlled testing system

3 Results and Discussion

The results of the experimental work are discussed under five sub-topics: (1) microscopic observations, (2) uniaxial compressive strength (UCS), (3) elastic modulus (E), (4) stress–strain relations, and (5) macroscopic failure pattern. The values of UCS and E of each sample tested are summarized in Table 1. Besides, a normalized value in the following is defined as the ratio of a mechanical index after

Table 1 The values of UCS and E of each specimen tested

Sample no.	T (°C)	UCS (MPa)	E (GPa)
20-1	20	53.30	14.7
20-2	20	38.20	10.0
20-3	20	48.68	13.2
200-1	200	41.74	12.3
200-2	200	40.60	12.7
200-3	200	47.00	12.5
400-1	400	63.08	15.5
400-2	400	33.34	12.1
400-3	400	56.18	17.4
600-1	600	45.00	7.9
600-2	600	33.77	7.2
600-3	600	35.75	8.3
800-1	800	20.32	2.1
800-2	800	16.48	2.4
800-3	800	19.90	2.3
1000-1	1000	15.60	1.2
1000-2	1000	8.05	0.8
1000-3	1000	9.46	0.7

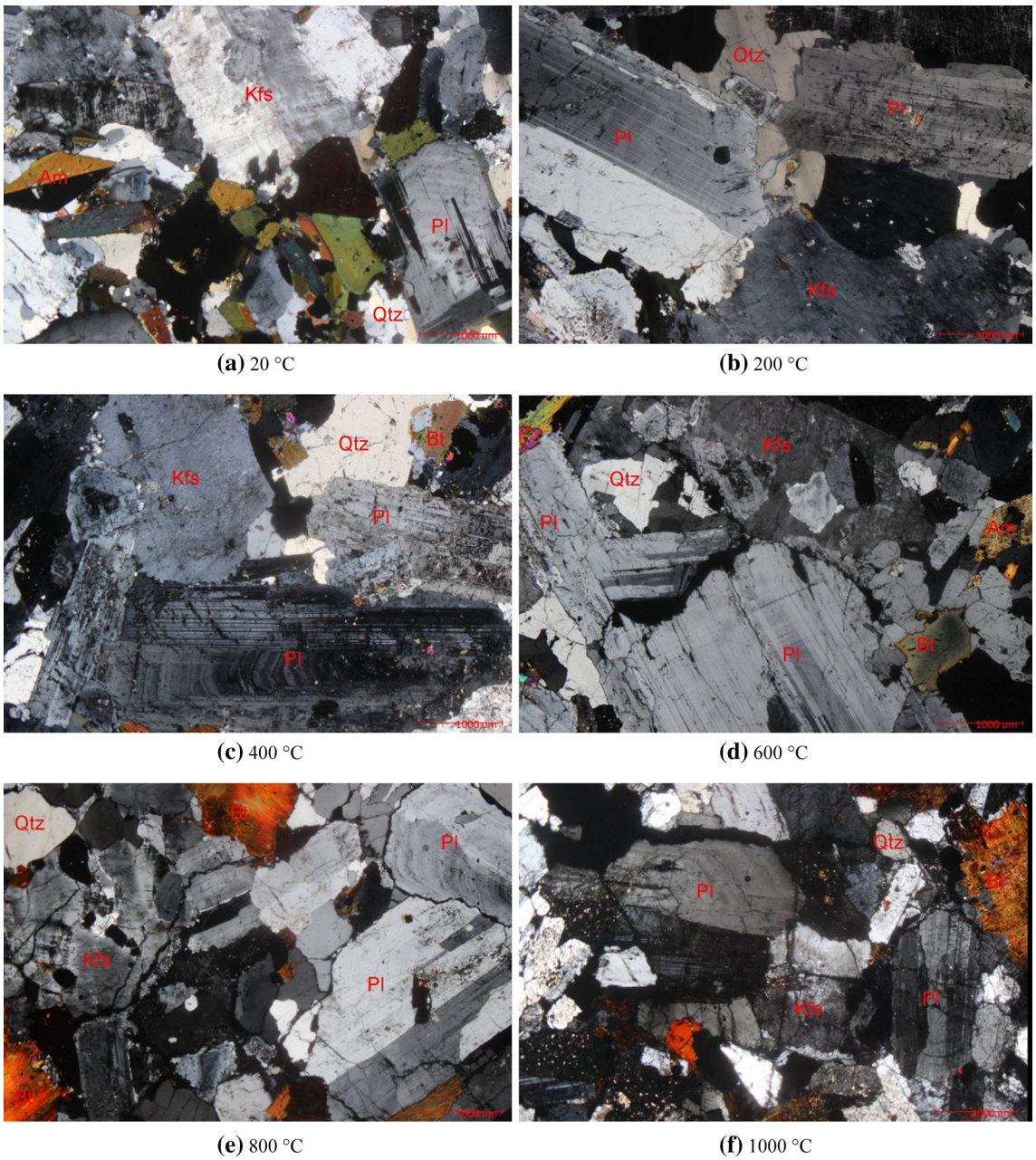

(a) 20 °C **(b)** 200 °C

(c) 400 °C **(d)** 600 °C

(e) 800 °C **(f)** 1000 °C

Fig. 2 Optical microscopic observations of the specimens after high temperatures

a specific temperature treatment to that at room temperature which is 20 °C in this study.

3.1 Microscopic Observations

Figure 2 illustrates the optical microscopic observation results in the diorite after different temperatures by thin section identification method, from which we can clearly see the influence of high temperature on the mineral grains and micro-cracks. Mineral grains are closely arrayed, and almost no initial pores and fissures can be observed at 20 °C (Fig. 2a). Short fissures appear around mineral boundaries, but not through the grains at 200 and 400 °C (Fig. 2b, c). At 600 °C, we can observe many boundary cracks and trans-granular cracks (Fig. 2d). More and more cracks have formed at 800 and 1000 °C, as shown in Fig. 2e, f.

3.2 Uniaxial Compressive Strength

UCS is one of the most important parameters reflecting the basic mechanical properties of rocks. It is extremely essential in the fields such as rock mass classification and development of rock and rock mass failure criteria (Jaeger et al. 2007). As listed in Table 1, clearly the measured

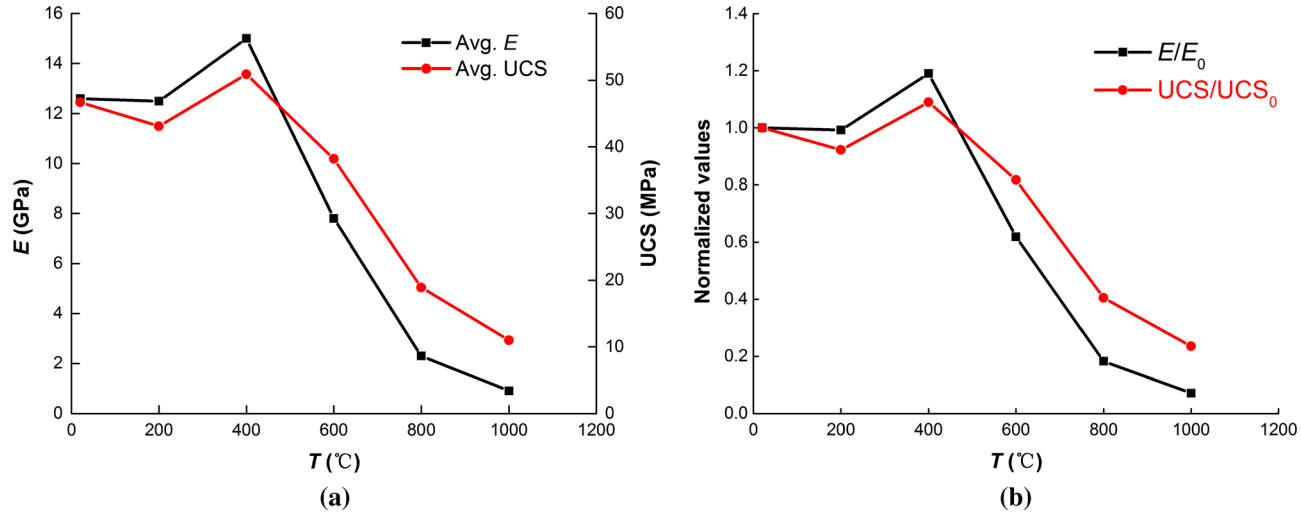

Fig. 3 **a** Average values of E and UCS versus temperature, **b** the normalized values versus temperature

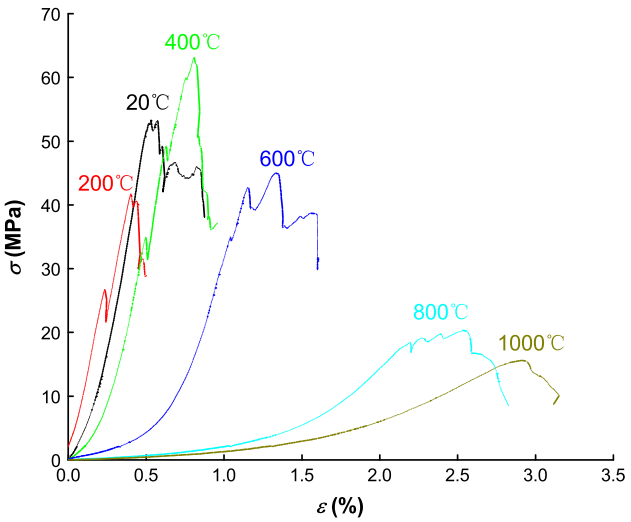

Fig. 4 Diorite stress–strain curves at different temperatures

values are distributed scatteredly (Fig. 3a), which have been observed in rocks whether they were experienced thermal treatment or not (e.g., Basu et al. 2013; Tian et al. 2014) and may be due to sample variations related to the amount and distribution of micro-cracks, microstructure, etc. The average values of UCS at each temperature are plotted in Fig. 3a and the corresponding normalized values UCS/UCS_0 in Fig. 3b. A general trend is obviously shown in Fig. 3, that is, slight variations (±10%) of UCS appeared up to 400 °C; from that onward, a decreasing trend was observed. UCS of the diorite decreases by approximately 60 and 80% after 800 and 1000 °C treatment, respectively. Microscopic observations have found thermally damaged cracks develop from 600 °C onward, and as a result, the macroscopic strength is affected significantly and presents a decreasing trend with temperature.

3.3 Elastic Modulus

As shown in Fig. 3, the values of E remain nearly unchanged from room temperature to 200 °C, but a slight increase (<20%) occurs at 400 °C. From 400 °C onward, E dramatically decreases with increasing temperature. At 800 and 1000 °C, the average values of E decrease by about 82 and 93%, respectively, compared to that at room temperature. The magnitude of E/E_0 variation with temperature from 400 to 1000 °C is larger than that of UCS/UCS_0 (Fig. 3b). It is concluded that high-temperature influence on elastic modulus is more obvious that on UCS in this temperature range.

3.4 Stress–Strain Relations

The axial stress–axial strain curves of representative tests at each temperature level considered are plotted in Fig. 4. We can see that the curves of 20, 200, 400, 600, 800, and 1000 °C show two different behaviors. The stress–strain curves of 20–400 °C display a nearly elastic increase in stress with strain until peak stress is reached and then a sudden drop of stress. The behavior indicates that diorite experiences brittle failure in this temperature range. On the other hand, the curves of the temperatures from 600 °C onward exhibit an obvious concave-upward shape before the elastic increase in stress with strain and a more gradual decrease in stress after peak stress with increasing strain at failure, reflecting the ductility of diorite is enhanced. The concave-upward shape indicates that the high temperatures have induced micro-cracks in the samples. Tullis and Yund (1987) experimentally demonstrated a transition from dominantly micro-cracking to dominantly dislocation at about 300–400 °C for quartz and 550–650 °C for feldspar. Moreover, the values of UCS of the diorite samples did not significantly vary (less

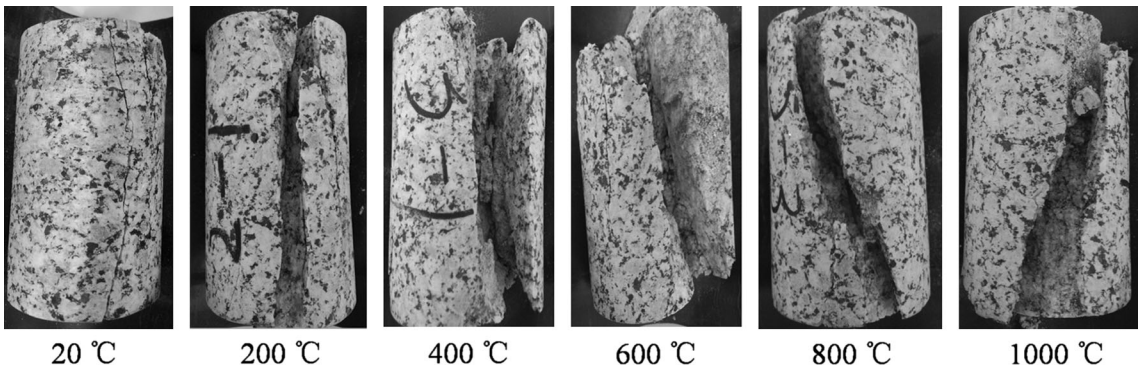

Fig. 5 Macro-fractures of diorite exposed to temperatures after uniaxial compression

than 20%) before 600 °C. Therefore, it can be concluded that the brittle–ductile transition critical temperature of diorite is around 600 °C, which is consistent with the conclusion of granite by Liu and Xu (2015). However, Xu et al. (2009) and Shao et al. (2015) presented the brittle–ductile transition temperature of granite is about 800 °C. This phenomenon is understandable, for mineral composition and microstructures of rocks are different (Ranjith et al. 2012).

3.5 Macroscopic Failure Pattern

The macroscopic failure patterns of diorite after high-temperature treatment are shown in Fig. 5. The diorite at room temperature is a typically brittle rock material and shows an axial splitting tensile failure pattern. After 200 and 400 °C treatment, there is a tendency to transit from a longitudinal splitting to shear failure. From 600 °C onward, failure of the specimens occurred along a through-going shearing plane, that is, shear failure. Besides, due to thermally damaged micro-cracks inside the specimens before compression, the failure planes of the specimens thermally treated are very hackly, and some blocks and powder come out. The phenomenon strengthens with increasing temperature. Longitudinal splitting and shear failure are normal failure pattern of rocks without thermal treatment under low pressures (Goodman 1980). After thermal treatment, especially beyond 400 °C, even though the stress–strain curves reflect the ductility of the samples is enhanced with temperature, the diorite still behaves a macroscopic shear failure pattern, which is consistent with the observations (see, e.g., Maji 2011; Kong et al. 2016; Yang et al. 2017).

4 Conclusions

A laboratory program to investigate the mechanical behavior of diorite exposed to high temperatures up to 1000 °C has been carried out. From the results of this study, the following conclusions can be drawn.

- Thermally damaged cracks such as boundary and transgranular cracks in the diorite treated occur obviously from 600 °C onward, corresponding to the fact that UCS and elastic modulus become less than those at 20 °C.
- The values of UCS of diorite change slightly (±10%) up to 400 °C, but decrease with increasing temperature from that onward.
- The elastic modulus of the diorite keeps unchanged up to 200 °C, increases about 20% at 400 °C compared to that of the original sample, and then decreases with temperature from 400 °C onward.
- Based on the stress–strain curves, the brittle–ductile transition critical temperature of the diorite is around 600 °C.

Acknowledgements The work is jointly supported by the National Natural Science Foundation of China (Nos. 51541405, 41602374, and 11602235).

References

Basu A, Mishra DA, Roychowdhury K (2013) Rock failure modes under uniaxial compression, Brazilian, and point load tests. Bull Eng Geol Environ 73(3):457–475

Brown DW, Duchane DV, Heiken G et al (2012) Mining the earth's heat: hot dry rock geothermal energy. Springer, Berlin

Burton E, Friedmann J, Upadhye R (2006) Best practices in underground coal gasification. Lawrence Livermore National Laboratory, Livermore

Chen YL, Shao W, Zhou YC (2012) Experimental study on the influence of temperature on the mechanical properties of granite under uni-axial compression and fatigue loading. Int J Rock Mech Min Sci 56:62–66

Ding Qh, Ju F, Mao XB et al (2016) Experimental investigation of the mechanical behavior in unloading conditions of sandstone after high-temperature treatment. Rock Mech Rock Eng 49(7):2641–2653

Dwivedi RD, Goel RK, Prasad VVR, Sinha A (2008) Thermo-mechanical properties of India and other granites. Int J Rock Mech Min Sci 45:303–315

Gelet R, Loret B, Khalili N (2012) A thermo-hydro-mechanical coupled model in local thermal non-equilibrium for fractured HDR reservoir with double porosity. J Geophys Res 117(B7):1–23

Goodman RE (1980) Introduction to rock mechanics. Wiley, New York

Homand-etienne F, Houpert R (1989) Thermally induced microcracking in granites: characterization and analysis. Int J Rock Mech Min Sci Geomech Abstr 26(2):125–134

Jaeger JC, Cook NGW, Zimmerman RW (2007) Fundamentals of rock mechanics, 4th edn. Blackwell Publishing, Hoboken

Kong B, Wang EY, Li ZH et al (2016) Fracture mechanical behavior of sandstones subjected to high-temperature treatment and its acoustic emission characteristics under uniaxial compression conditions. Rock Mech Rock Eng 49(12):4911–4918

Liu S, Xu JY (2014) Mechanical properties of Qinling biotite granite after high temperature treatment. Int J Rock Mech Min Sci 71:188–193

Liu S, Xu JY (2015) An experimental study on the physic-mechanical properties of two post-high-temperature rocks. Eng Geol 185:63–70

Maji VB (2011) Understanding failure mode in uniaxial and triaxial compression for a hard brittle rock. In: Zhou YX (ed) Harmonising rock engineering and the environment. Taylor & Francis Group, London, pp 336–337

Otto C, Kempka T (2015) Thermo-mechanical simulations confirm: temperature-dependent mudrock properties and nice to have in far-field environmental assessments of underground coal gasification. Energy Procedia 76:582–591

Peng J, Rong G, Cai M et al (2016) Physical and mechanical behaviors of a thermal-damaged coarse marble under uniaxial compression. Eng Geol 200:88–93

Ranjith PG, Viete DR, Chen BJ et al (2012) Transformation plasticity and the effect of temperature on the mechanical behaviour of Hawkersbury sandstone at atmospheric pressure. Eng Geol 151:120–127

Sellin P, Leupin OX (2013) The use of clay as an engineered barrier in radioactive-waste management—a review. Clay Clay Miner 61(6):477–498

Shao SS, Ranjith PG, Wasantha PLP et al (2015) Experimental and numerical studies on the mechanical behaviour of Australian Strathbogie granite at high temperatures: an approach to geothermal energy. Goethermics 54:96–108

Singh B, Ranjith PG, Chandrasekharam D et al (2015) Thermo-mechanical properties of Bundelkhand granite near Jhansi, India. Geomech Geophy Geo-Energy Geo-Res 1(1):35–53

Tian H, Ziegler M, Kempka T (2014) Physical and mechanical behavior of claystone exposed to temperatures up to 1000°C. Int J of Rock Mech Min Sci 70:144–153

Tian H, Kempka T, Xu S et al (2016) Mechanical properties of sandstones exposed to high temperature. Rock Mech Rock Eng 49:321–327

Tullis J, Yund RA (1987) Transition from cataclastic flow to dislocation creep of feldspar: mechanisms and microstructures. Geology 15(7):606–609

Verma AK, Gautam P, Singh TN et al (2015) Discrete element modeling of conceptual deep geological repository for high-level nuclear waste disposal. Arab J Geosci 8:8027–8038

Xu XL, Kang ZX, Ji M et al (2009) Research of microcosmic mechanism of brittle-plastic transition for granite under high temperature. Procedia Earth Planet Sci 1(1):432–437

Yang SQ, Ranjith PG, Jing HW et al (2017) An experimental investigation on thermal damage and failure mechanical behavior of granite after exposure to different high temperature treatments. Geothermics 65:180–197

Yin TB, Shu RH, Li XB et al (2016) Comparison of mechanical properties in high temperature and thermal treatment granite. Trans Nonferr Met Soc China 26:1926–1937